Wafer-scale Ge epitaxial foils grown at high growth rates and released from porous substrates for triple-junction solar cells

Peer-reviewed author version

DEPAUW, Valerie; Porret, Clement; Moelants, Myriam; Vecchio, Emma; Kennes, Koen; Han, Han; Loo, Roger; Cho, Jinyoun; Courtois, Guillaume; Kurstjens, Rufi; Dessein, Kristof; Orejuela, Victor; Sanchez-Perez, Clara; Rey-Stolle, Ignacio & Garcia, Ivan (2023) Wafer-scale Ge epitaxial foils grown at high growth rates and released from porous substrates for triple-junction solar cells. In: PROGRESS IN PHOTOVOLTAICS, 31 (12), p. 1315-1328.

DOI: 10.1002/pip.3634
Handle: http://hdl.handle.net/1942/38934

Wafer-scale Ge epitaxial foils grown at high growth rates and released from porous substrates for triple-junction solar cells

Valérie Depauw[*1, 2, 3] 0000-0003-2045-9698
Clément Porret[2] 0000-0002-4561-348X
Myriam Moelants[2]
Emma Vecchio[2]
Koen Kennes[2]
Han Han[2] 0000-0003-2169-8332
Roger Loo[2] 0000-0003-3513-6058
Jinyoun Cho[*4] 0000-0002-3524-1256
Guillaume Courtois[4] 0000-0003-0865-7405
Rufi Kurstjens[4] 0000-0003-4482-3052
Kristof Dessein[4] 0000-0002-9440-270X
Víctor Orejuela[5] 0000-0003-3361-6509
Clara Sánchez-Pérez[5] 0000-0003-3291-8601
Ignacio Rey-Stolle[5] 0000-0002-4919-5609
Iván García[5] 0000-0002-9895-2020

* | Corresponding authors: valerie.depauw@imec.be & jinyoun.cho@eu.umicore.com
1 | University of Hasselt, imec-imomec, Hasselt, Belgium
2 | imec, Leuven, Belgium
3 | EnergyVille, Genk, Belgium
4 | Umicore, Electro-Optic Materials, Olen, Belgium
5 | Universidad Politécnica de Madrid, Instituto de Energía Solar, Madrid, Spain

Abstract

Germanium is listed as a critical raw material and, for environmental and economic sustainability reasons, strategies for lower consumption must be implemented. A promising approach are Ge lift-off concepts, which enable to re-use the substrate multiple times. Our concept is based on the Ge-on-Nothing approach that is the controlled restructuring at high temperature of a macro-porous Ge surface, forming a Ge foil weakly attached to its parent wafer. Its suitability as III-V epitaxy seed and support substrate has previously been demonstrated with proof-of-concept solar cells. This work focuses on bringing this concept to the next level, by upscaling the detachable area to a full 200-mm wafer scale, increasing foil thickness for sufficient light absorption in the Ge bottom cell, and improving the control on the strength that is bonding the suspended foil to its parent. By introducing a new high growth-rate epitaxy process from $GeCl_4$, and by engineering the GeON structure to introduce pillars with ad-hoc density and shape, we fabricated P-type foils with tunable boron doping up to 15 µm in thickness and 11 cm × 11 cm in area, for which the detachment strength could be adapted to

the stresses induced by the solar cell process steps. The surface roughness and the electrical and crystal qualities of these foils were inspected by AFM, SIMS, SRP, ECCI and TEM to check the $GeCl_4$-based epitaxy conditions, and to check that the ad-hoc pillars were not introducing any damage. Small-area triple-junction lattice-matched GaInP/GaInAs/Ge solar cells were fabricated on 7-µm-thick Ge foils with various pillar densities and on a standard reference Ge wafer. The III-V layer nucleation was virtually the same on both substrates and the solar cells on the GeON foils performed in the same way as the cells on the Ge wafer, albeit a small loss in short-circuit current and open-circuit voltage that can be attributed to the thickness reduction and absence of rear-side passivation. We conclude that it is possible to gain control on the GeON detachability and upscale the concept to areas relevant for the space PV industry, proving that porous germanium is a serious candidate for replacement of bulk Ge wafers in view of a more sustainable multijunction solar cell process.

Keywords

Germanium, lift-off, epitaxy, multijunction solar cells

1 | Introduction

Germanium (Ge) is today's workhorse substrate for III-V based multijunction solar cells for space applications, for which it fulfills the three functions of (1) seed for III-V heteroepitaxy, (2) mechanical support for device processing and (3) bottom junction. But Ge is a heavy, expensive, and critical raw material [1]. Environmental and economic sustainability, especially in the current context of a potentially expanding market, are both calling for bottom-up approaches for thinner and flexible substrates with lower Ge consumption. A wide range of approaches is being considered, which either lift-off thin Ge foils from a Ge wafer or avoid using Ge at all by lifting-off III-V foils from gallium arsenide (GaAs) wafers, or by growing on alternative substrates such as silicon (Si). The III-V layer quality on silicon wafers or virtual Ge substrates [2]–[5] is far from being on par with GaAs and Ge. If in the future, progress could be expected from remote epitaxy [6], the currently most advanced approaches are the epitaxial lift-off (ELO) technique, spalling and release from porous germanium [7].

The porous germanium approach could supply waste-free Ge substrates with tunable thickness, fulfilling the three functions that thick Ge wafers are currently ensuring. Strengths of this approach are its high potential for achieving defect-free and smooth epi-ready surfaces with

high throughput and detachment yield, with the extra advantage that the concept has already been demonstrated at industrial level with porous silicon [8], [9]. Two routes of porous germanium are currently under development, based on random mesopores or patterned macropores. The former is usually referred to as “porous Ge” and the latter as “GON” or “GeON” [10], [11]. Porous Ge is fabricated by electrochemical etching and is potentially the lower cost route [12], [13]. The GeON structure involves lithography and dry etching but provides easier control on the detachment layer and seed surface morphology. It also can be applied to any wafer doping and results in a perfectly non-porous seed. The GeON approach for waste-free germanium substrates is illustrated in **Figure 1.** Its core mechanism is the controlled restructuring of macroporous Ge at high temperature forming a so-called Ge-on-Nothing (GeON) structure, a suspended membrane attached by a few anchor points to the wafer. The suspended foil thickness is directly determined by the pore pitch and diameter [14]. A practical limit is set by the anneal time and temperature that are necessary to ensure the Ge surface diffusion for complete pore closure and merging and can be estimated around 5 µm [15], which is on the low side for a Ge bottom cell in a typical multijunction solar cell to absorb enough infra-red light [16]. This thickness can thus further be increased by epitaxial growth. Both thickness and doping of this Ge layer can be tuned by homoepitaxy as required by the solar cell design. Provided the epitaxial deposition growth rate is high enough, the foil may be thick enough (beyond a range 20-100 µm depending on the cell process and handling methods) for free-standing processing. Underneath, the highly porous layer is engineered to avoid its delamination during processing or cracking during layer transfer. After device fabrication and detachment, the Ge wafer is reconditioned and reused multiple times.

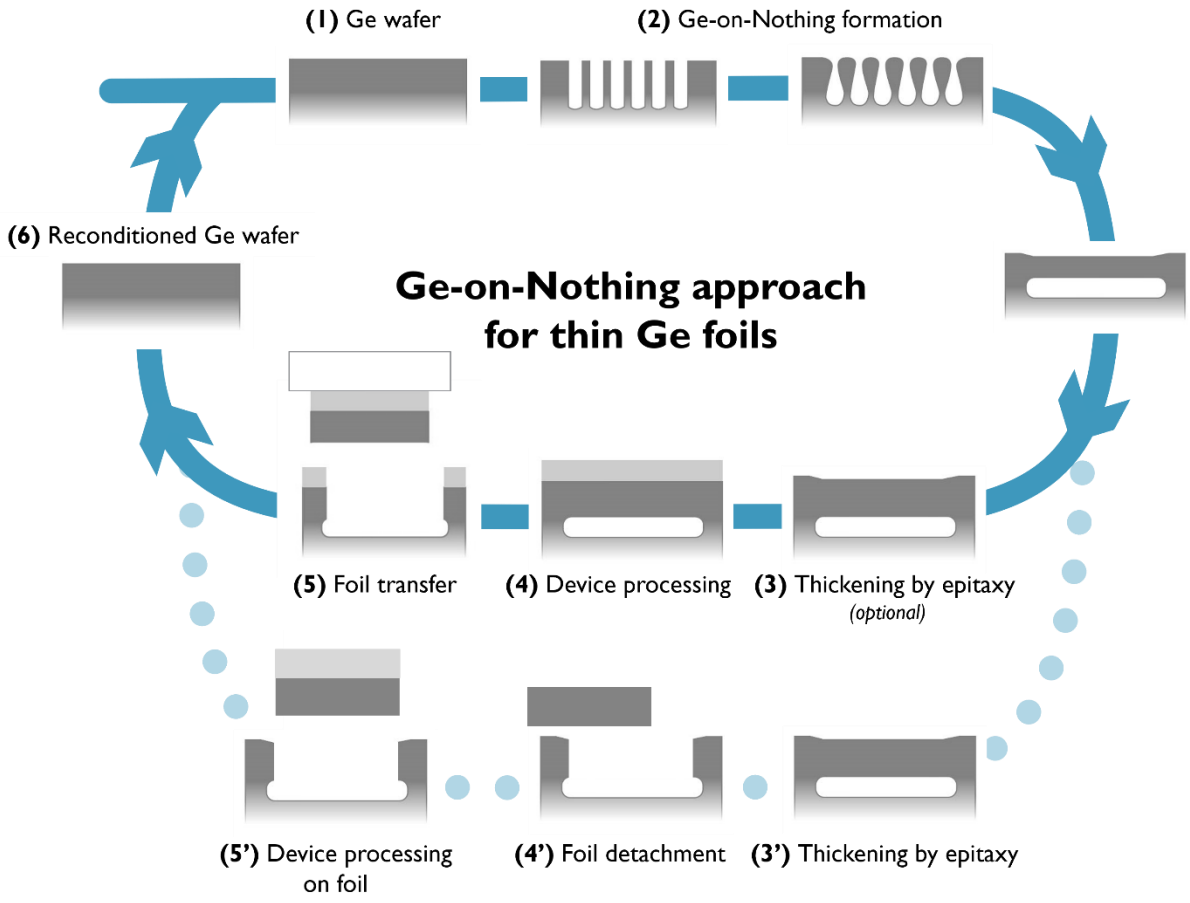

Figure 1 | Ge-on-Nothing approach: (1) a Ge wafer is (2) porosified with regular macropores which are transformed into a suspended defect-free seed layer enabling epitaxy of (3) Ge and (4) high-quality III-V layers, and eventually (5) their transfer to a carrier substrate, while (6) the Ge wafer is reused. The Ge seed may be grown thick enough for free-standing processing, without support from the Ge wafer (3', 4', 5').

The proof-of-concept of the GeON approach (exclusive of wafer re-use) was demonstrated in 2019 by Park et al. for III-V solar cells on small areas [10], using nanoimprint lithography and dry etching. Here we extend the demonstration for the other two key Ge wafer functions of support substrate and bottom cell. The paper is structured following the three main steps of the GeON process, and the relevant experimental details are given at the start of each section. In Section 2, we upscale the GeON foil area to a wafer scale and identify a way to adapt the layer detachability to the requirements of the solar cell process. In Section 3, we demonstrate that the foil can be thickened with epitaxy from $GeCl_4$ at a growth rate up to 190 nm/min (and possibly more). In Section 4, we fabricate detachable triple-junction solar cells with the Ge foil as bottom cell, reaching similar performance as with a standard wafer reference.

2 | From Ge wafer to wafer-scale detachable Ge foil

The second function that Ge wafers should fulfill for fabricating space solar cells is that of supporting substrate for the III-V thin films. The void structure that is formed below the Ge wafer with the GeON concept must be engineered to enable transferring the solar cell at the adequate moment, and this must be achieved defect-free over the whole wafer scale.

2.1 | Experimental: GeON formation and foil transfer

For GeON wafer fabrication, a 200-mm 6º offcut Ge wafer was patterned by deep-UV lithography and dry-etched (**Figure 2 a**) to form an array of straight columnar pores. The GeON areas of the wafer were defined at the lithography stage and various wafer layouts could be defined by stepping the mask, from ~ 0.9 cm × 0.8 cm zones to a full wafer exposure. The layout in the figure is an example with 12 areas of 2.5 cm × 2.5 cm fitting within a 150-mm-diameter disk. O_2 dry- and 2% HF wet-etching were used to strip and clean the surface. The patterned wafer was then loaded in a load-locked chemical vapor deposition reactor where an annealing step in a reducing environment (730 ºC at 1 atm H_2) restructured the surface in a few minutes, resulting in a GeON structure with a perfectly closed surface (**Figure 2 b**). The foil was optionally thickened in-situ by epitaxial growth in conditions detailed in Section 3. The foils were then transferred either manually to a Gel-Pak® or to a glass substrate by adhesive bonding. For the former, a Gel-Pak® with strength 'X4' was simply manually stuck and peeled from the wafer surface, with the GeON foil transferred on (**Figure 2 c**). For bonding to glass, two different methods were tested. For both, a 700-µm glass substrate Corning SG 3.4 was coated with the adhesive 305 from Brewer Science with a 1-cm edge-bead removal (EBR). In the first method, the GeON wafer was bonded in a manual EVG520 bonder at 180 ºC with force applied with force applied at room temperature and kept for the whole thermal cycle. This led to a crack in the glass and wafer at the edge, initiated outside of the GeON area, which was assigned to several coating defects in the adhesive layer. The glass/GeON-wafer stack was then blade-diced within the edges of the GeON area and the two substrates were (lightly) pulled apart manually. In the second method, bonding was done in an automated XBS300 temporary bonder from Süss Microtec at 200 ºC with force applied after the bonding temperature was reached and debonding was performed manually with a razor blade (no blade dicing was needed since the GeON area covered the whole bonded area). No glass or wafer cracking was then observed.

The foils were visually inspected under a halogen lamp and with optical and scanning-electron microscopy (SEM). The SEM image of a GeON wafer with a suspended 16-µm-thick foil is shown in **Figure 2 d**. A SEM (SEM-Vision from AMAT) was also used to follow the evolution of specific defects which could be located by their coordinates.

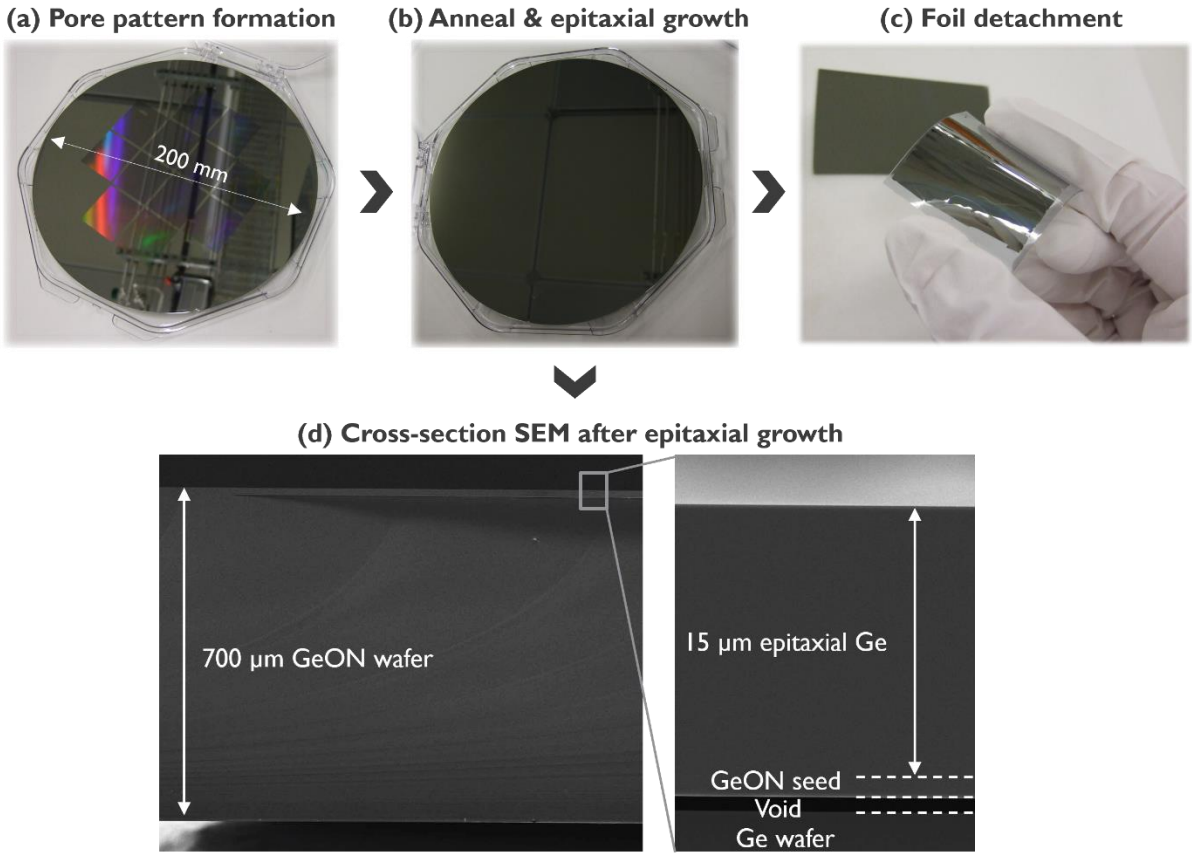

Figure 2 | Photographs of a 200-mm Ge wafer processed into a GeON wafer: (a) Twelve areas are defined by lithography and dry etching; (b) annealing and epitaxial growth transform them into smooth, now mirror-polished surfaces, with the GeON areas becoming barely visible by eye; (c) one of the 16-µm-thick foils is peeled off with an adhesive polymer; (d) Cross-section SEM of a GeON wafer with a 15 µm epitaxial foil.

2.2 | Upscaling the foil area

Detached GeON foils of a few mm^2 were reported in 2019 by Park et al. [10]. In 2020, 2.5 cm × 2.5 cm detached areas were demonstrated by Courtois et al. [11]. Solar cells were fabricated in 2021 but only on non-detachable GeON surfaces [17]. The next step is upscaling beyond 100-mm and 150-mm diameter wafers (the common wafer dimensions for the space PV industry), and for which two hurdles are faced. The first, practical, hurdle is that the Ge foil dimensions are limited by the lithography and dry-etch tool resolution, uniformity, and reproducibility. The tools must enable a sufficient process control to keep pore dimensions within a window of tolerance for pores to be able to merge. Or, failing that, pores should form interruptions in the merged void that will be small enough to break during detachment without

affecting the foil integrity. We observe that small punctual defects, i.e., affecting less than ~ 10 pores, are normally not a concern. Such defects will form, for example, at crystal originated pits (COP) smaller than a couple of micrometers in diameter, because these depressions are out-of-focus for deep-UV lithography, preventing proper resist exposure and pore opening (**Figure 3**). The lithography process tolerance can, to a certain extent, be enlarged by playing with the illumination conditions. In our case, the depth-of-focus could be pushed up to 1.5 µm. This means that the entire GeON area must fall within a plane +/- 750 nm, setting strict limits for the wafer site-flatness quality requirement (SFQR). In zones falling outside of that focus plane, pores do not form or merge properly, preventing foil detachment and resulting in large holes and/or cracks. The larger the GeON area, the higher the chance of encountering a point or area that will fall out of focus. If 200-mm Si wafers can meet this SFQR and below (130 nm standard for deep-UV), this is not yet the case for 200-mm Ge wafers that are not an industry standard. Still, exposure was upscaled to the full 200-mm wafer, including the wafer edges (**Figure 4 a)**, where more out-of-focus zones can be found. The impact of such out-of-focus zones is illustrated with a particularly defected 19-cm diameter wide GeON foil, featuring both edge and center defects (**Figure 4 b, c)**.

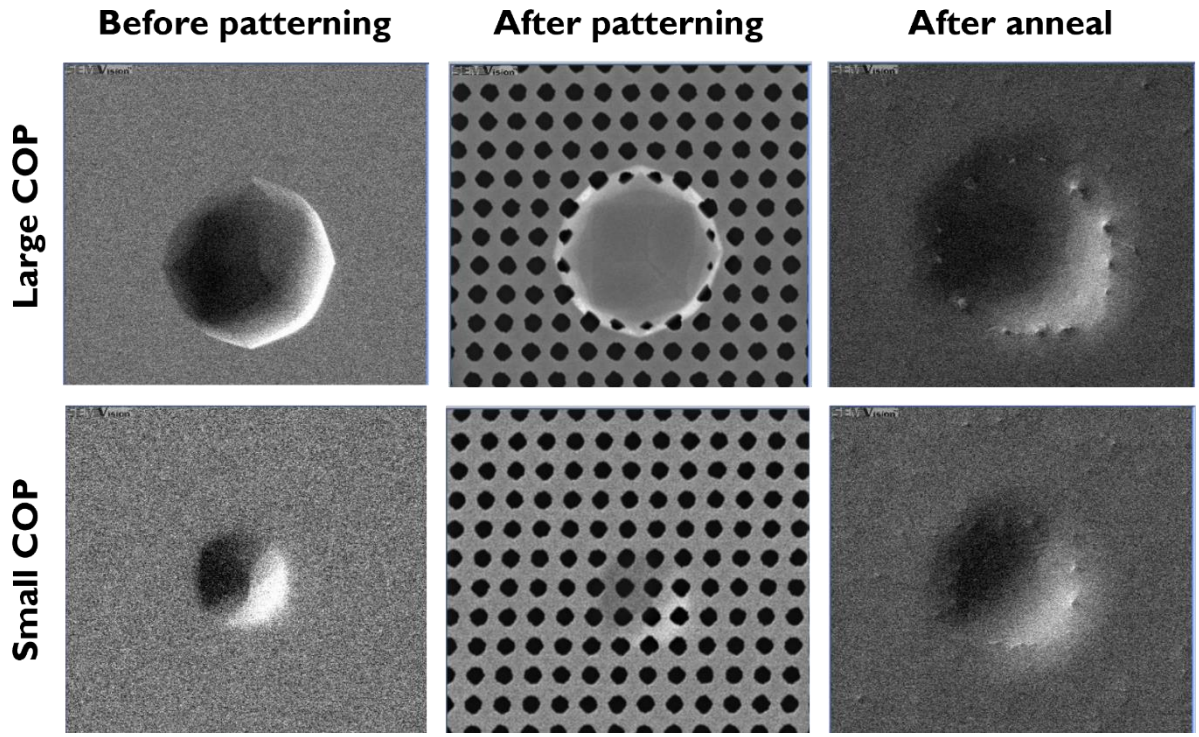

Figure 3 | Top-view SEM images at the location of two crystal-originated pits (COP) of the evolution of the GeON surface along the process, from the starting blanket surface up to pore reorganization. Only the large COP prevented pore formation, but both eventually led to an interruption in the detachment layer, a pillar.

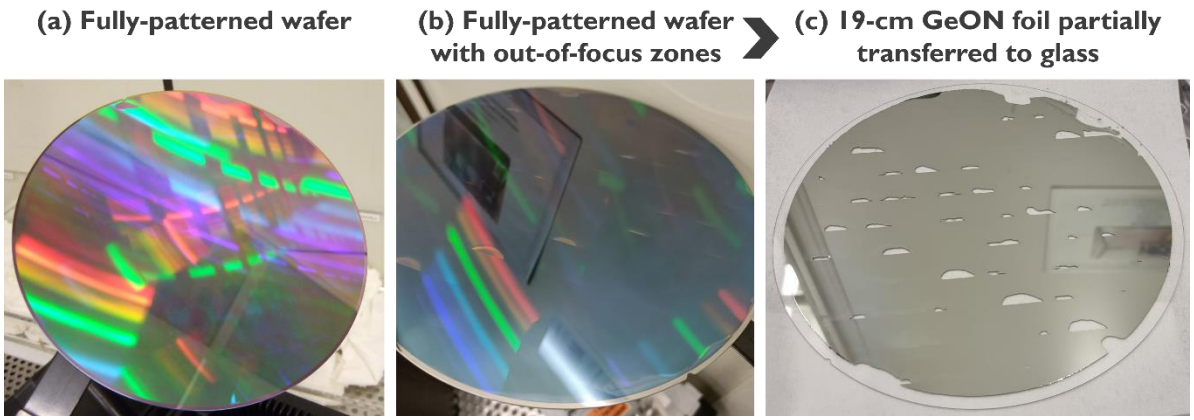

Figure 4 | Photographs of (a) a 200-mm Ge wafer patterned with macropores across the whole surface, with only a few defects at the edges from out-of-plane exposure in contrast to a wafer featuring defects across the whole surface due to insufficient SFQR. (c) These defects led to holes in the 1-µm thick GeON foil after transfer by adhesive bonding to a glass substrate.

There is yet a second hurdle in upscaling the foil area, that is not depending on the process conditions but that is inherent to the GeON concept itself, and which relates to the foil sagging under its own weight and pressure differences between the ambient and the void. This aspect was discussed for silicon in [14]. If the foil bends down sufficiently to touch the parent wafer, while the temperature is yet high enough for atoms to bond, the void locally annihilates. Annealing the foil at atmospheric pressure is a first means to limit sagging. Besides, in practice, and over areas beyond the millimeter scale, random pillars form. They can withstand the foil provided their density is high enough. How to control this density is the object of the next section. The successful formation of a complete 11 cm × 11 cm foil, diced within a 12 cm × 12 cm GeON area, is shown in **Figure 5**. The foil was chipped by blade-dicing on one edge but was otherwise hole-free.

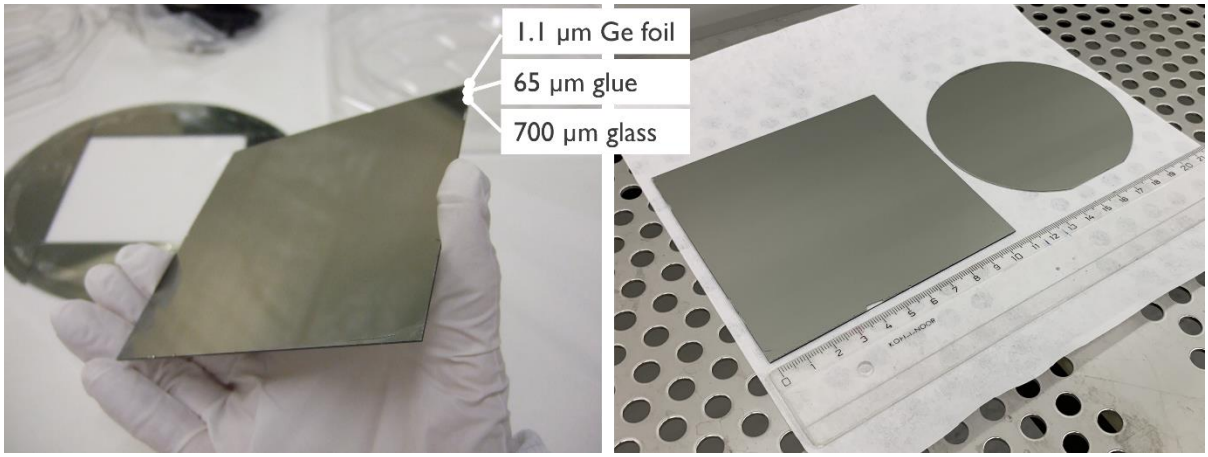

Figure 5 | GeON foil of 1.1 µm thickness transferred to a 11 cm × 11 cm glass substrate via adhesive bonding, demonstrating lift-off of an area larger than a 100-mm-diameter wafer.

2.3 | Controlling detachability

The porous structure must result in a GeON wafer with an epi-ready surface sufficiently resilient to be used as a Ge wafer equivalent for III-V hetero-epitaxy. Previously, we demonstrated GaInP solar cells on GeON wafers, but not yet detached solar cells [17]. For this purpose, the foil must feature a density of pillars that appropriately trades off ease of detachment (i.e. weak enough to be compatible with standard bonding methods) and resistance to delamination (i.e. strong enough to withstand the mechanical stress from the ambient variations caused by e.g. pressure, temperature, and from the foreign solar cell materials themselves). GeON zones featuring low pillar density can easily blister and eventually flake, even as early as directly upon unloading from the epitaxial reactor (**Figure 6 a**). The pillar density that is appropriate to maintain the foil pinned and stable (**Figure 6 b**) naturally depends on the stresses that it will have to undergo in the following stages. The higher the stresses, the higher the required pillar density.

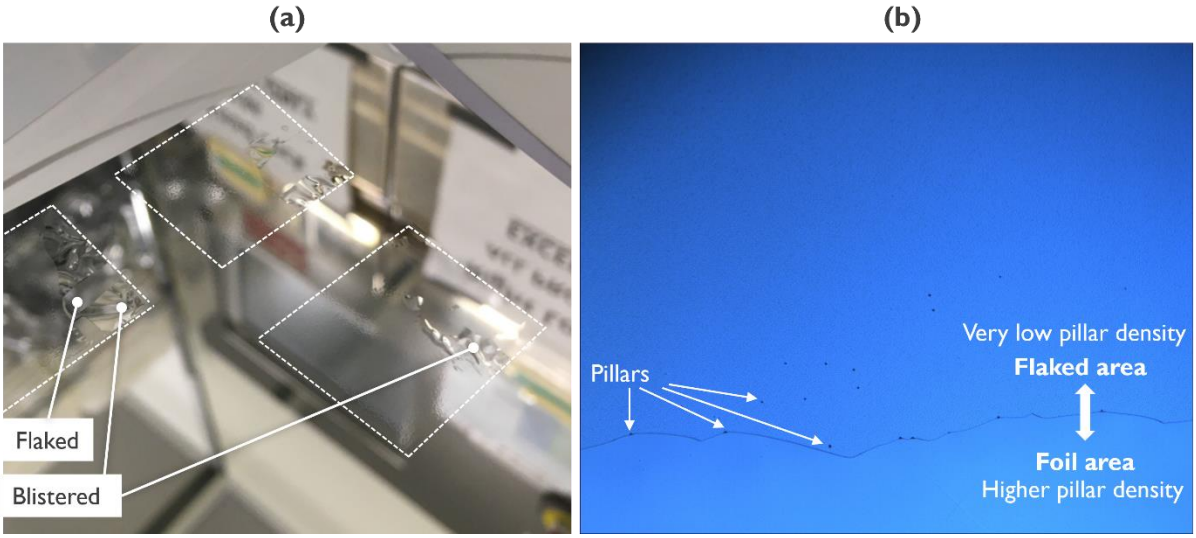

Figure 6 | (a) Photograph of three 2.5 cm × 2.5 cm foils with 1 µm epitaxial Ge and random pillars unloaded from the epitaxial reactor that partly blistered and flaked; (b) top view optical microscope image of a foil at the edge of a flaked zone, showing how pillars are pinning the foil to the parent wafer.

As explained in the previous section, pillars tend to form at random locations, with a density determined by the porous structure (porosity, wall profile, surface chemistry) and thermal profile and ambient [15]. The interplay between these many parameters and the difficulty in controlling germanium surface ageing make it very difficult to achieve a reproducible and uniform random pillar density. Instead, ad-hoc pillars were introduced by designing a new lithography mask including modifications to the pore pattern and design. Different types of irregularities (which cannot be disclosed here for intellectual property reasons) were introduced

with different pitches in the periodic pore pattern of the lithography mask. In total, 12 + 6 combinations of pillar types and densities were tested with low-force adhesive bonding, with a Gel-Pak® plastic foil (**Figure 7**). Pillars of 4 types were either full or hollow and with different diameters, while their pitches explored a range of detachment force up to a factor 5000. The reference pitch is the lowest and is labeled as "F1", with "F5000" corresponding to a 5000 times higher detachment force. A first screening of pillar pitch was performed with multiplication factors 1, 25, 100 and 400 and compared to random pores. Foils were tested both with and without 1 µm of Ge epitaxial thickening. Detachment results (**Figure 7**) confirmed that both pillar pitch and dimensions are parameters that can be used and combined to control detachability. For instance, hollow pillars (labeled as type #2 in the figure) for a given pitch F400 could be detached while bulkier types (types #1, 3, 4) could not [18]. Interestingly, the density of random pillars seemed to significantly drop below a determined pillar pitch, restricting interferences from random pillars on these detachment tests. Further investigations would be needed to confirm this observation and improve our understanding of pillar formation.

In a second screening, new combinations exploring larger pillar densities (detachment forces 100, 200, 1500 and 5000 times higher), were prepared and tested for non-thickened foils in various processes mimicking the cell fabrication (long annealing beyond 600 ºC in the hetero-epitaxy reactor, lithography, metallization by thermal evaporation or plating, ...). Densities F200 and beyond, that did not show any sign of alteration, namely flaking, cracking, blistering at macroscopic or microscopic levels, were chosen for fabricating solar cells (Section 4).

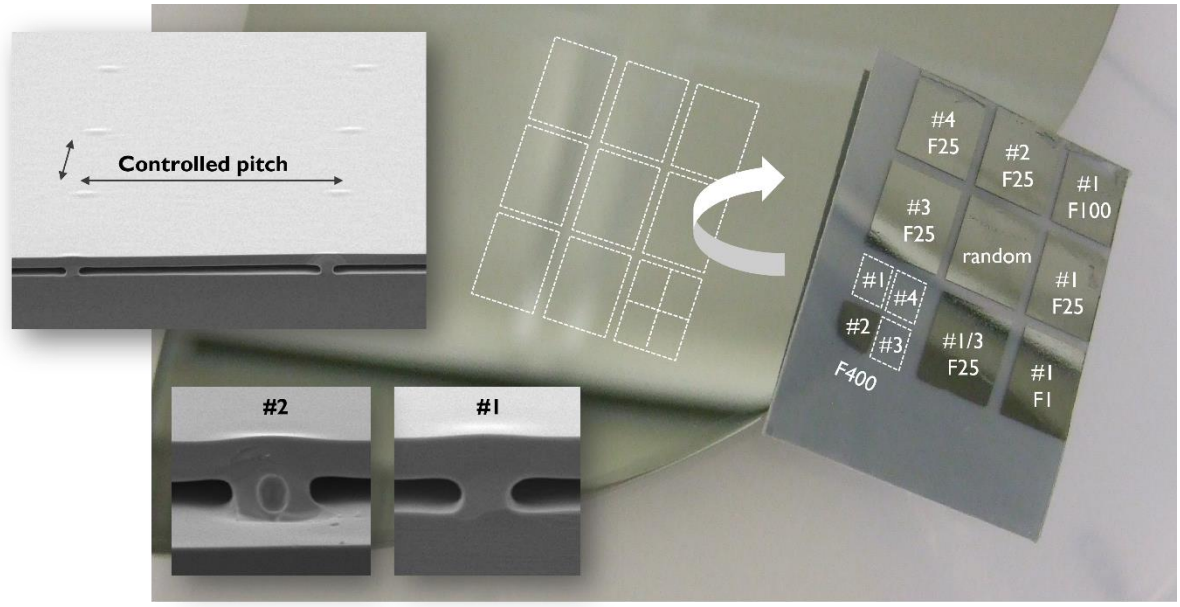

Figure 7 | Photographs of 12 GeON areas (9 mm × 9 mm) with 4 different pillar pitches (SEM image in upper inset, with detachment force multiplication factors F of 1 to 400) and types (e.g. SEM images of #1 and #2 in lower insets), amongst which 9 were transferred to Gel-Pak®. The 3 areas with smallest pitch and largest pillar dimensions were too strongly attached.

3 | From 1-µm up to 30-µm-thick GeON foil with high growth-rate epitaxy

The third function that Ge wafers should fulfill for high efficiency multijunction solar cells is that of bottom cell. Since the thickness of the GeON seed layer is limited to a few micrometers [15], it requires thickening up if no advanced light trapping schemes are implemented [19]. Thickening can be done in-situ by homoepitaxy right after reorganization. To maximize growth rates, a new process with $GeCl_4$ as precursor [20] was developed. Finding appropriate growth conditions on a GeON seed could however be challenging because this microstructure is expected to keep evolving above 550 ºC. Thermal budget and reactor pressure variations must therefore be minimized to avoid foil collapse and void annihilation, while maximizing growth rate and keeping a high-quality dislocation-free III-V epi-ready surface.

3.1 | Experimental: epitaxial growth and foil characterization

Ge epitaxial growth processes were developed using several test-vehicles such as 200 mm Si wafers with patterned oxide stripes and Ge / Si virtual substrates [21]–[24]. The growth process took place in an ASM Epsilon® 2000 system, which is a horizontal, cold wall, single wafer, load-locked CVD epi reactor. $GeCl_4$ was used as Ge precursor [20] and benchmarked with conventional GeH_4. H_2 was used as carrier gas. Compared to GeH_4, $GeCl_4$ limits parasitic deposition on the reactor cold walls and hence enables the controlled growth of µm-thick films

while reducing the frequency of tool maintenances. In a later stage, boron doping was introduced using B_2H_6 (1% diluted in H_2) as a dopant source. Differential mass and step height measurements (on wafers with oxide stripes) were used to determine the deposited thickness and process uniformity. Micro 4-point probe (M4PP) measurements were employed to extract sheet resistances and material resistivities. Nomarski optical microscopy was used to check the surface morphology and high-resolution X-ray diffraction (HRXRD) was used to check the material structural properties. Selected conditions were finally applied to Ge bulk wafers and GeON foils [25].

Various characterization methods were used to check the Ge foil quality. In this case, dopant concentrations were confirmed by secondary ion mass spectrometry (SIMS) and spreading resistance probe measurements (SRP). SIMS measurements were performed in a Cameca IMS-ScUltra magnetic sector instrument. Cs^+ and O^+ primary beams were used at 4 keV and 2 keV impact energy respectively. Concentrations were calibrated by relying on qualified homogeneously-implanted Ge references. The depth scales were calibrated from crater depth measurement. At the top surface and interfaces, SIMS artefacts will be present and may result in the quantification deviating from real level. The crystal quality was evaluated by transmission electron microscopy (TEM) and electron channeling contrast imaging (ECCI). A beam voltage of 20 kV and a beam current of 1.6 nA were used with a working distance of 5 mm to acquire ECPs with an angular range of around 5°. Areas of 533 μm^2 were inspected. The TEM lamellas were prepared after spin-on carbon and platinum capping, lifted-out at one of the pillars by focused ion beam (FIB) and positioned on a copper grid. TEM was implemented at 200 kV in a Cs-corrected Titan system under different bright field (BF) conditions to visualize different crystalline defects, and scanning TEM (STEM) in annular dark field (ADF), annular bright field (ABF) and high-angle annular dark field (HAADF) modes. ECCI measurements were performed in a Thermo Scientific Apreo SEM system. A retractable annular solid-state semiconductor detector was situated between the pole piece and the sample to collect the backscattered electrons (BSE). Finally, surface roughness was measured with an atomic force microscope (AFM) in tapping mode.

3.2 | Reaching high growth-rates with $GeCl_4$

Initial results from Ge epitaxial growth processes offering high throughputs were already presented in [26]. Ge epitaxy was performed at atmospheric pressure and a temperature of 550°C, to operate in the mass-transport limited regime where growth rates are maximized (**Figure 8**). By increasing the $GeCl_4$ precursor flow, growth rates up to ~ 190 nm/min could be

demonstrated, without clear saturation - suggesting faster depositions may still be possible - nor observable degradation of material morphology (via SEM) and structural properties (using XRD). This is to be compared with the growth rate of ~ 40 nm/min typically achievable using GeH_4 in our hardware setup. This enabled the growth of ~ 15 µm Ge films with an acceptable deposition time of ~ 75 min. Detachable foils up to 30 µm could also be grown in two epitaxy steps, to include a tube etch step in between to limit the thickness of the Ge layer deposition on the susceptor.

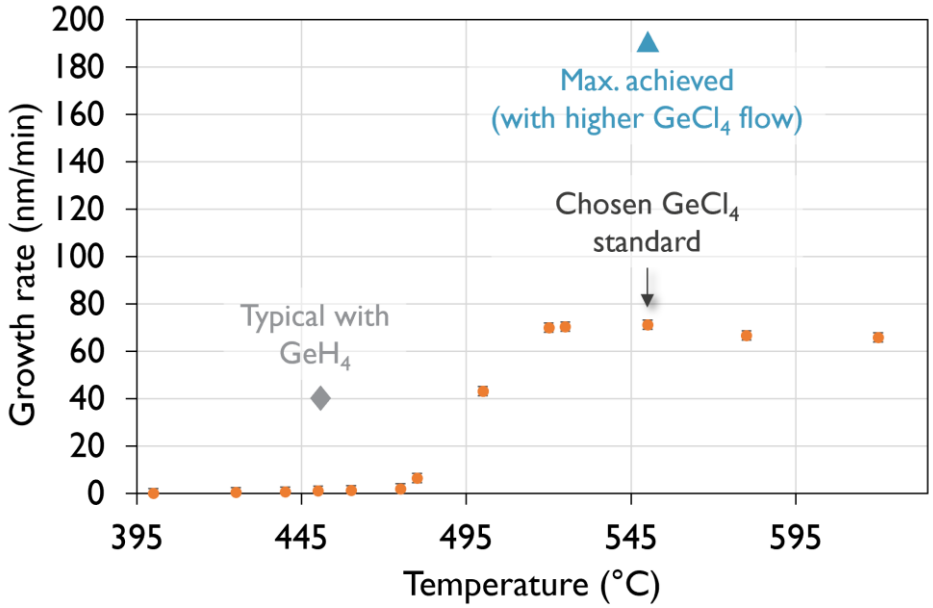

Figure 8 | Ge growth rate as a function of growth temperature. Ge depositions were performed on Si substrates, at atmospheric pressure. The deposition time was set to 5 minutes. The mass-transport limited regime is reached from temperatures of 520°C on. For comparison, two other growth rates achieved with different conditions are indicated: our typical growth rate with GeH_4 and the maximum achieved with higher $GeCl_4$ precursor flow.

Following initial growth rate assessments, boron-doping was investigated with a view to forming the bottom junction of the final solar cell. Screening several B_2H_6 precursor flows allowed to vary the B doping concentration from 3.10^{17} cm^{-3} to $1.3.10^{19}$ cm^{-3} with full dopant activation, as confirmed by M4PP and SIMS measurements. This data showed controllable and tunable doping levels across 2 orders of magnitude and was used as a process calibration for epitaxial growth on GeON foils. Some results are detailed in the next section.

3.3 | Epitaxial Ge foil quality

After setting a reference process on blanket Si and Ge wafers, depositions were started on GeON wafers. The quality of the $GeCl_4$-thickened foils grown on GeON seeds with regular pillars influencing their topography, was evaluated in complementary ways to check their suitability as bottom solar cell. Firstly, cross-section SEM inspections were done to verify that

the foil was not collapsed and sealed after processing for more than 1 hour at 550 ºC. The void structure was still present and no change in pillar dimension could be noticed, showing that the GeON structure could survive these conditions of epitaxial thickening.

Then, minority-carrier lifetime measurements were performed and were reported in detail in [26]. The effective lifetime measured in 16-µm-thick intrinsic layers (3 cm × 3 cm passivated on both sides with hydrogenated amorphous silicon) grown on p-type GeON wafers reached reasonable values around 25 µs. These foils were grown with a pillar density F25, which enabled manual detachment with Gel-Pak® adhesive but could still sustain the two surface passivation steps by plasma-enhanced chemical vapour deposition, in vacuum.

Thirdly, the dopant concentration and activation in foils with various boron levels were measured by secondary-ion mass spectroscopy (SIMS) and spreading resistance probe (SRP). The SIMS profile of a 10-µm-thick boron-doped epi-layer ([B] = 4.10^{18} cm^{-3}) grown on a gallium-doped GeON wafer ([Ga] = 3.10^{17} cm^{-3}) is shown in **Figure 9**. The drop in germanium intensity around 12 000 nm indicates the GeON void interface. The epitaxial foil above shows a sharp interface with the GeON seed. A light depletion of Ga down to ~ 2.10^{17} cm^{-3} at the top surface of the 1 µm GeON seed layer can be noted, probably caused by dopant desorption during the restructuring step in hydrogen at 730 ºC. A comparison of chemical and active doping concentrations on two different samples showed an acceptable match and a complete dopant activation with [B] = $2.5.10^{18}$ cm^{-3} by SIMS against [hole] = 4.10^{18} cm^{-3} by SRP, and [B] = $1.8.10^{19}$ cm^{-3} against [hole] = $1.3.10^{19}$ cm^{-3}.

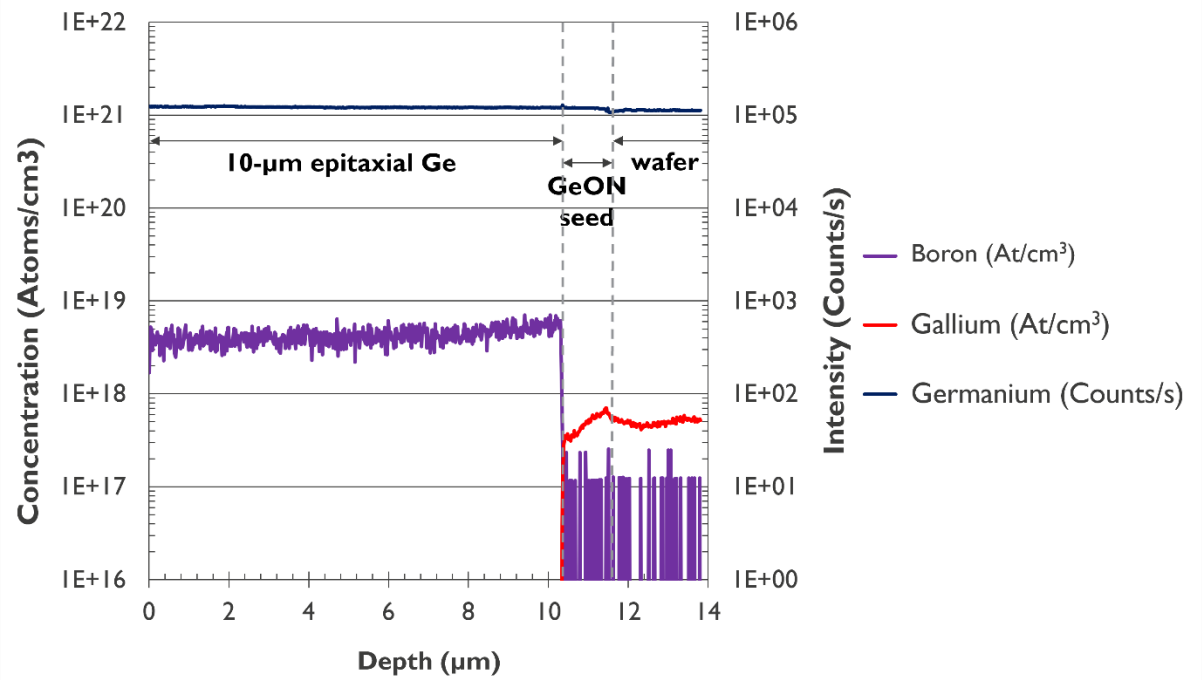

Figure 9 | SIMS depth profiles of a boron-doped 10.5-µm-thick epitaxial layer grown on a gallium-doped GeON wafer. The interface between the Ga-doped wafer and the B-doped epi-layer is abrupt while the top-surface of the GeON seed layer shows a Ga depletion.

The composition of the GeON seed layer was further investigated with higher sensitivity to light elements within a thinner epitaxial foil. This time the boron-doped layer was grown on a phosphorous-doped wafer in two steps of 500 nm, with unloading of the epitaxial reactor and storage in the N_2 load-lock in between. This two-step deposition was performed to see the impact of a reload on the epitaxy quality. The SIMS profile (**Figure 10**) reveals three aspects of the GeON process. Firstly, interfacial boron and oxygen spikes are detected between the two layers at 500 nm depth. This allows to visualize the portions grown in the two epitaxial growth steps. It is yet unclear if this interface has an impact on the electrical quality. Apart from these two spikes, the boron concentration is stable and on target, and the oxygen level at the background level (detection limit). Secondly, the GeON formation process is confirmed to induce a light dopant depletion at its front surface, both for phosphorous and gallium (**Figure 9**). Thirdly, if inside the GeON, oxygen and carbon stay below the background limits, it is not the case in the wafer surface. The porous structure visibly gettered oxygen and carbon contaminations to the wafer surface. These impurities may have been present in the starting substrate or, more probably, may have been incorporated along the pore walls during the lithography and dry-etching processes, indicating that surface cleaning may require fine-tuning.

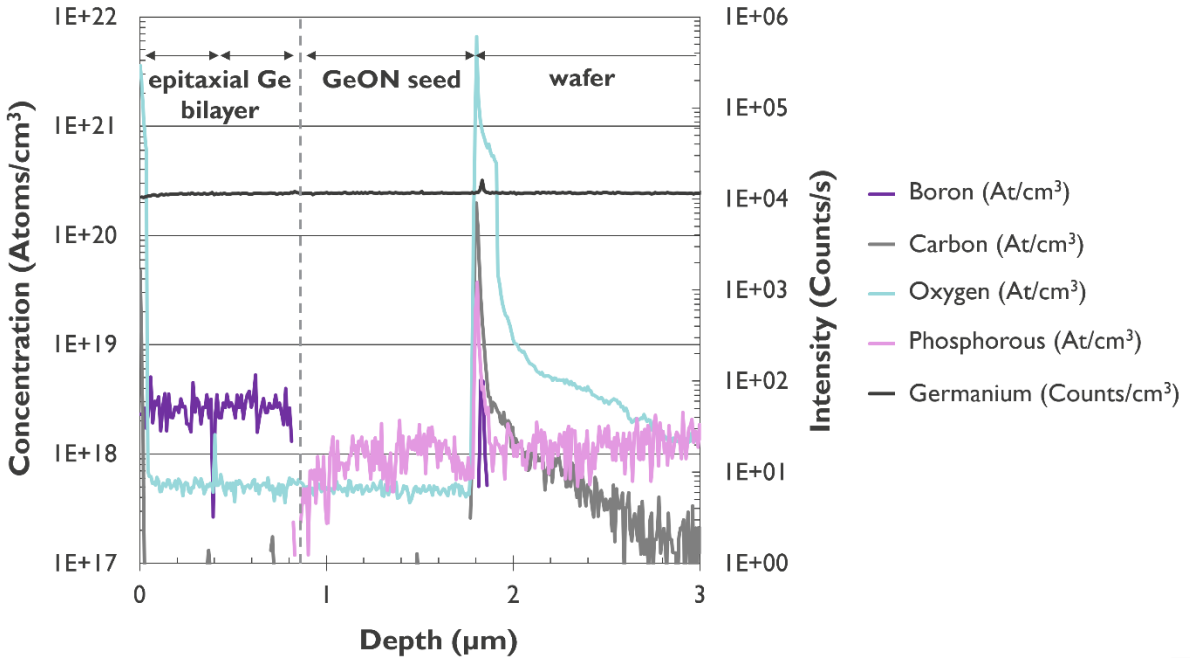

Figure 10 | SIMS depth profiles of GeON wafer with a 1-µm-thin B-doped epitaxial layer grown in two steps on a phosphorous doped wafer. Apart from a light P depletion in the GeON seed top layer, the two dopant concentrations are constant (within measurement noise). The interface between the two epitaxial layers is sensed and traces of O and C contamination are found below the Ge wafer surface. The sharp peaks at 0 and 1.8 µm depth are measurement artefacts.

The same sample with 1-µm epitaxy grown in two steps, with pillar density F25, was inspected by TEM and ECCI to check if pillar inclusion, and the two-step growth, impacted the crystal quality. Two pillars extracted from edge and center of the wafer were inspected by TEM, while at ECCI 16 pillars were inspected over two surfaces of 533 μm^2. No discontinuities or crystal defects were found by TEM - with an inspection in both 220 BF and 400 BF TEM, and STEM images in HAADF, ADF and ABF modes (**Figure 11**) - neither any threading dislocation (TD) by ECCI [27]. The absence of any TD on the inspected area - that is unfortunately limited by inspection time – lets us set an upper limit of $1.8.10^5/cm^2$. But from the fabrication method, no TD is actually expected on these samples.

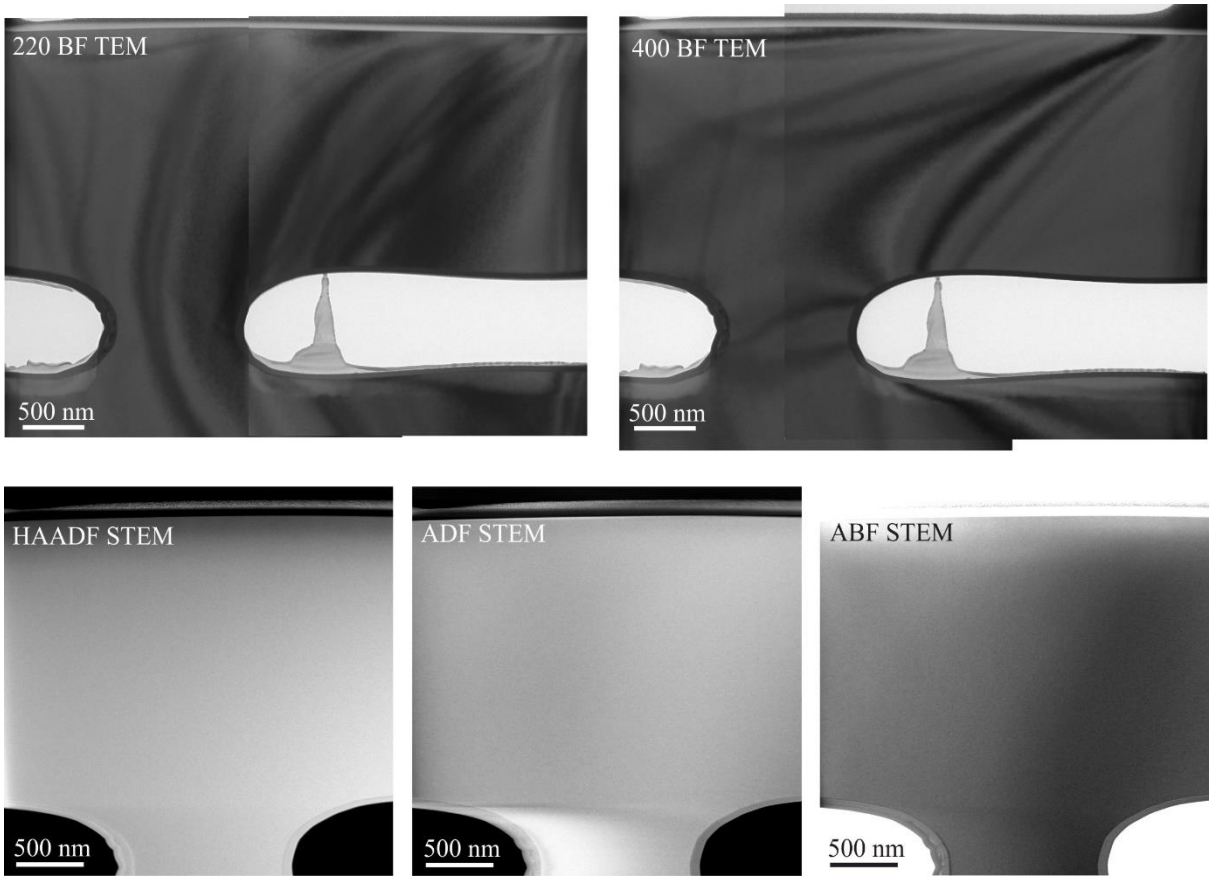

Figure 11 | TEM images in 220 and 400 BF and STEM images in HAADF, ADF and ABF modes, from which no discontinuity or crystal defect is observed (the interface between the GeON seed and the epitaxial layer being expected around the middle of the suspended layer). HAADF-STEM intensity is proportional to the thickness of the TEM specimen and to the averaged atomic number of the material in the e-beam while ABF- and ADF-STEM intensities are related to the density and crystallinity of the different layers. The contrasted zone within the void is an artefact from the lamella preparation.

The pillars did not affect the crystal quality, but they do impact the GeON topography since they locally perturbate the pore reorganization and formation of the buried void. The topography evolution at the pillar location was measured by atomic force microscopy (AFM) as a function of the epitaxial Ge thickness (**Figure 12**). The standard GeON topography presents a characteristic waviness, induced by the reorganization process. Typical surfaces are almost one order of magnitude rougher than an unprocessed epi-ready Ge wafer (~ 2 nm RMS for GeON vs. 0.2 nm RMS for epi-ready wafer). However, this type of roughness was previously found to be compatible with III-V epitaxy [11], [20]. Furthermore, the amplitude and granularity of this waviness are significantly smoothened out by the layer thickening in the present conditions, reaching ~ 0.7 nm RMS (**Figure 12 a-c**). At the location of pillars either protrusions or depressions are formed, depending on the type of irregularity that was introduced

in the pore pattern. Fortunately, Ge homoepitaxy is not significantly affected and reduces the height of the pillar-induced steps by 50% within 10 µm growth (**Figure 12 d-f**).

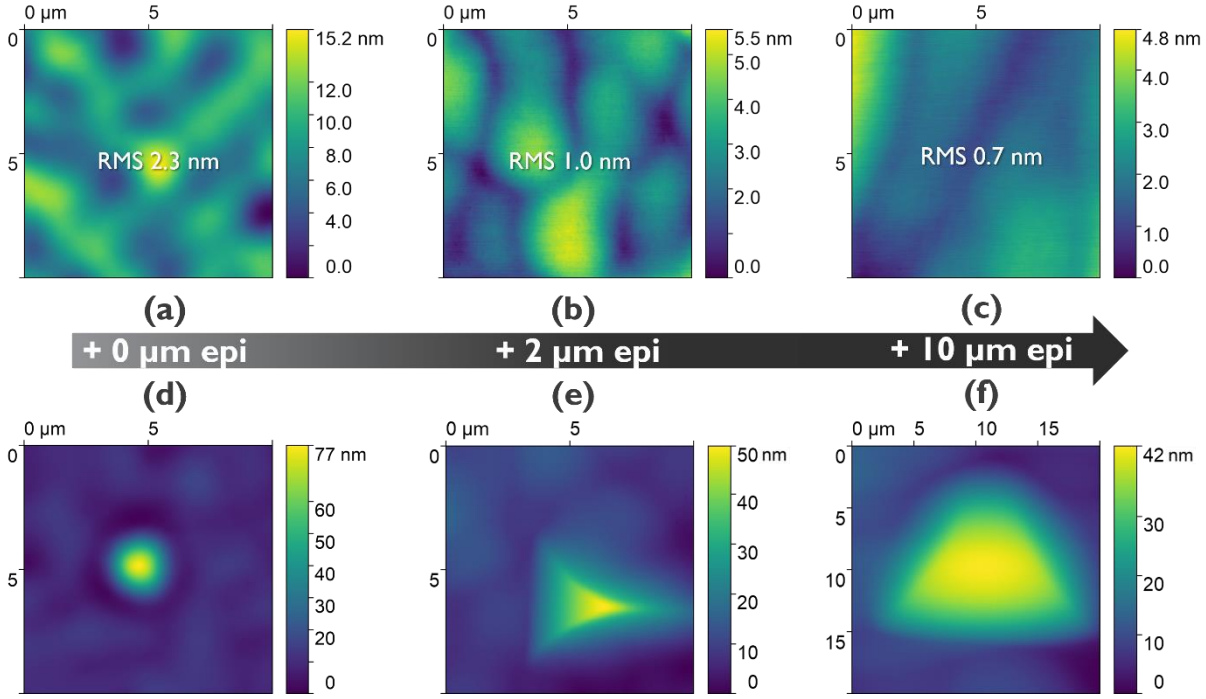

Figure 12 | (a-c) 10 µm × 10 µm atomic-force microscopy images with corresponding root mean square roughness for typical GeON surfaces with 0, 2 or 10 µm-thick Ge epitaxial thickening, showing that the thicker the epitaxial layer is, the smoother its topography becomes. (d-e) 10 µm × 10 µm and (f) 20 µm × 20 µm AFM images of pillars of type #1 for the corresponding epitaxial thickness.

In conclusion, the electrical, crystalline, and morphological quality of Ge foils grown from $GeCl_4$ by homoepitaxy on a GeON wafer including pillars seems suitable for growing multijunction solar cells with this foil as bottom cell. The fabrication of triple-junction solar cells is reported in the next section.

4 | From GeON foil to detachable triple-junction solar cell

4.1 | Experimental: solar cell fabrication

Triple-junction solar cell (3JSC) structures with Ge as bottom cell were grown on GeON samples with three different pillar densities with associated detachment forces, namely F200, F1500 and F5000. The Ge foil is 7 µm in all these samples and consists of a 6 µm B-doped Ge epilayer with [B] = 6.10^{17} cm^{-3} grown on a Ga-doped GeON wafer with [Ga] = 5.10^{17} cm^{-3}. The initially 200-mm round wafer was scaled down by laser to 7 cm × 7 cm and then by cleaving to ~ 2.5 cm × 2.5 cm for accommodation inside the epitaxial reactor and the plating tool. No prior cleaning step was performed. The structures comprise a GaInP nucleation layer

followed by GaInAs overbuffer as template onto which a GaInAs and GaInP subcells were grown connected by tunnel junctions, using a similar structure as described in [28]. The GaInAs middle cell is optically thick, while the GaInP top cell is thinned to approximate a current-matched structure for the AM0 solar spectrum. The total thickness of this III-V structure is ~5.5 µm. This semiconductor structure is deposited by metal-organic vapor-phase epitaxy (MOCVD) using an R&D AIX200/4 model reactor. The precursor gases used for group-V elements are AsH_3 and PH_3, while the group-III element precursors are TMGa, TMAl, TMIn. The doping of layers is achieved using DETe and DTBSi for n-type materials and DMZn and CBr_4 for p-type materials. An EpiRAS 2000-TT in-situ monitoring tool is used to measure the reflected spectral power and reflectance anisotropy spectra (RAS) during growth.
Solar cell devices with 0.1 cm^2 active area were fabricated using standard photolithography techniques and electroplated gold. The device isolation is achieved by wet etch of mesa trenches. The usual processing for 3JSC structures on standard Ge was used. No anti-reflection coating (ARC) was applied to these solar cells. It is important to note that the preparation of the samples prior to the MOCVD growth, which included laser dicing, produced particles across the GeON area. The particle density was not high enough to have any detectable effect on the in-situ measurements during MOCVD growth, or to dramatically affect the performance of the final solar cell devices but produced shunts of varying importance in some of them. Besides, the samples, after dicing, also had to undergo shipment but their non-standard dimensions prevented following the normal “safe” packaging procedure for Ge wafers to limit risk for surface ageing.

In addition to the in-situ measurements commented above, the surface morphology of the structures was characterized by optical microscopy with Nomarski optics. The lattice-matching was measured by rocking curves taken using high-resolution X-ray diffractometry (HRXRD) in a Panalytical X’Pert Pro tool (data not shown here). All structures are grown lattice-matched to the Ge or GeON substrate at growth temperature. This implies a slight compressive lattice-mismatch at room temperature.

It should be noted that the GeON samples did not show any issues during the growth of the 3JSC structures or the solar cell fabrication processes, such as cracking due to the thermal load and delamination of the Ge foils after metallisation. For these steps, that involved some wet processing (e.g. spin coating, solvent dip, electroplating) or thermal stresses (e.g. hotplate bake

or MOCVD) the lowest pillar density F200 was therefore sufficient. Other conditions, such as III-V epitaxy conditions involving lattice mismatch and stronger strain (i.e., in upright metamorphic solar cell designs), may require a larger pillar density but could not yet be tested.

The solar cells performance was characterized by measuring their I-V curves in the dark and under illumination in a Xe-lamp solar simulator, with no spectrum correction, with the Ge foils still attached to the Ge parent wafer. The spectral response was measured using a custom-built system based on a Xe-lamp light source and a monochromator. The fluctuations in the spectral irradiance of the light source were monitored using a GaInAs detector. The lock-in technique is used for a high signal-to-noise ratio, by chopping the light beam at 257 Hz. In order to light bias the junctions during measurement of the subcells in the 3JSC, MIGHTEX's high power LEDs of wavelengths 530 nm, 740 nm and 940 nm for top, middle and bottom junctions, respectively, were used. The voltage bias required was achieved by using the appropriate function in the Stanford Research Instruments SR570 preamplifier.

4.2 | Triple-junction solar cell results

We first look into the nucleation of III-V material on the Ge surface, by comparing standard Ge substrates and GeON samples. **Figure 13** shows the RAS signature during GaInP nucleation on these samples. As can be observed, the shape of the signatures is virtually identical, indicating that no differences in the surface reconstruction during nucleation can be detected among these samples.

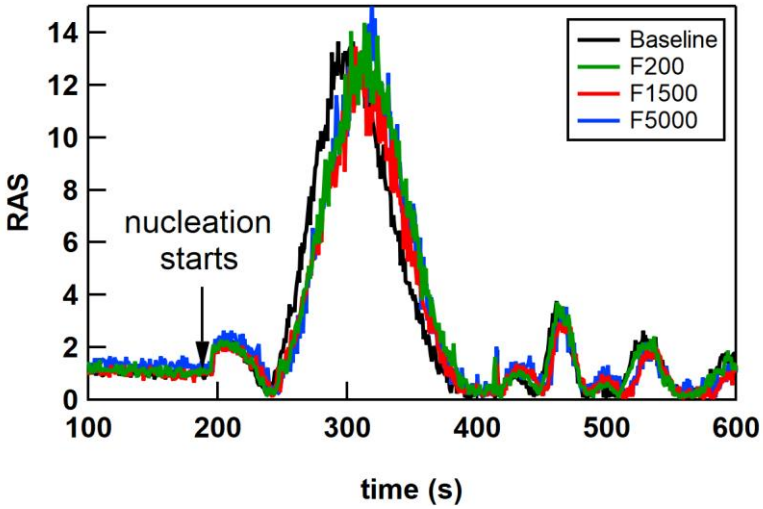

Figure 13 | RAS signature during nucleation of the GaInP layer on the Ge surface of a baseline standard Ge substrate and the GeON samples.

The external quantum efficiency (EQE) of finished 3JSC solar cell devices was measured. The solar cells used for this test had no front grid shadowing and no anti-reflection coating. The measurement results are shown in **Figure 14**. First, it can be appreciated that the GaInP top cell response is virtually identical in all the cases, within measurement uncertainty. This is indicative of the high quality of the Ge surfaces, given the fact that the GaInP material is the most sensitive to surface morphology problems among the materials used in the 3JSC. The response of the GaInAs middle cell shows a varying shape in the interference fringes, which is due to slight changes in the layer thicknesses. However, if we focus on the average level of the response, a lower value for the F200 sample can be observed. This sample exhibited uncontrolled ageing of the GeON surface during preparation of the samples, which caused some macroscopic defects during MOCVD deposition producing partial shunts in the solar cell devices. These shunts appeared to affect the response of the GaInAs middle cell. We expect, though, that the carrier collection efficiency in all the cases is virtually identical. Finally, the Ge bottom cell in the GeON samples shows a lower response in the long wavelength region as compared to the baseline, as corresponds to the lower Ge layer thickness: 7 µm in the GeON versus 170 µm in the baseline on standard Ge substrate. We expect that the photon reflection at the Ge/air interface at the back of the GeON samples is helping mitigate the reduction in the response by giving the light a second chance to be absorbed. Anyway, the response in all cases is higher than necessary for a Ge bottom cell in a 3JSC for space applications.

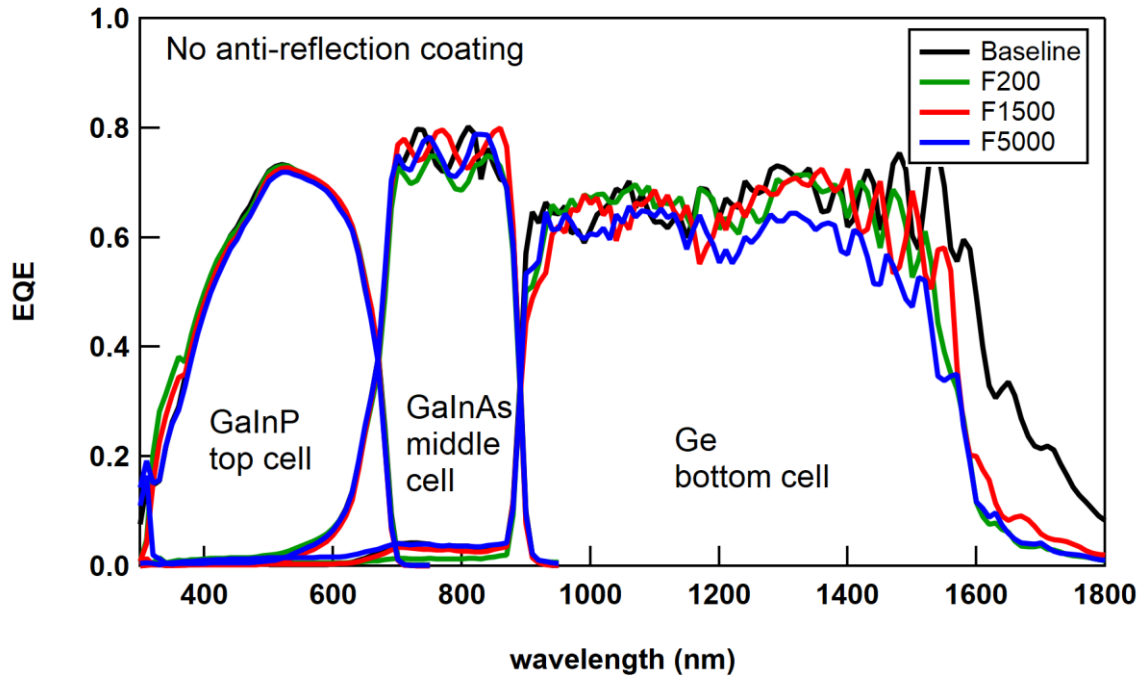

Figure 14 | EQE of 3JSC solar cells grown on a baseline standard Ge substrate and on the GeON samples. These solar cells have no anti-reflection coating.

Finally, I-V curves of the 3JSC solar cells were measured on a set of devices and are shown in **Figure 15**. The ~10 % dispersion observed in the short circuit current (I_{SC}) of the light I-V curves is mainly due to different shadowing factors in the devices. The comparison of the I_{SC} of baseline and GeON reveals similar values. The open circuit voltage (V_{OC}) shows a just slightly lower value in the 3JSC grown on GeON, by about 30 mV. This is better than expected, since the Ge bottom cell (just 7 µm thick) in these cells must be severely affected by a high back surface recombination, as compared to the case of standard Ge substrate (170 µm thick bottom cell). Moreover, the V_{OC} of the Ge subcell can be improved if its back surface is passivated after detachment from the parent substrate. The case of F200 sample shows a much lower V_{OC} due to the problem with Ge surface ageing commented upon before. It seems that the effect of the Ge surface degradation was such that the recombination pathways in the cells are different, as revealed by the significantly different ideality factor observed in the dark I-V curve. We believe this issue must be eliminated by preventing the surface degradation.

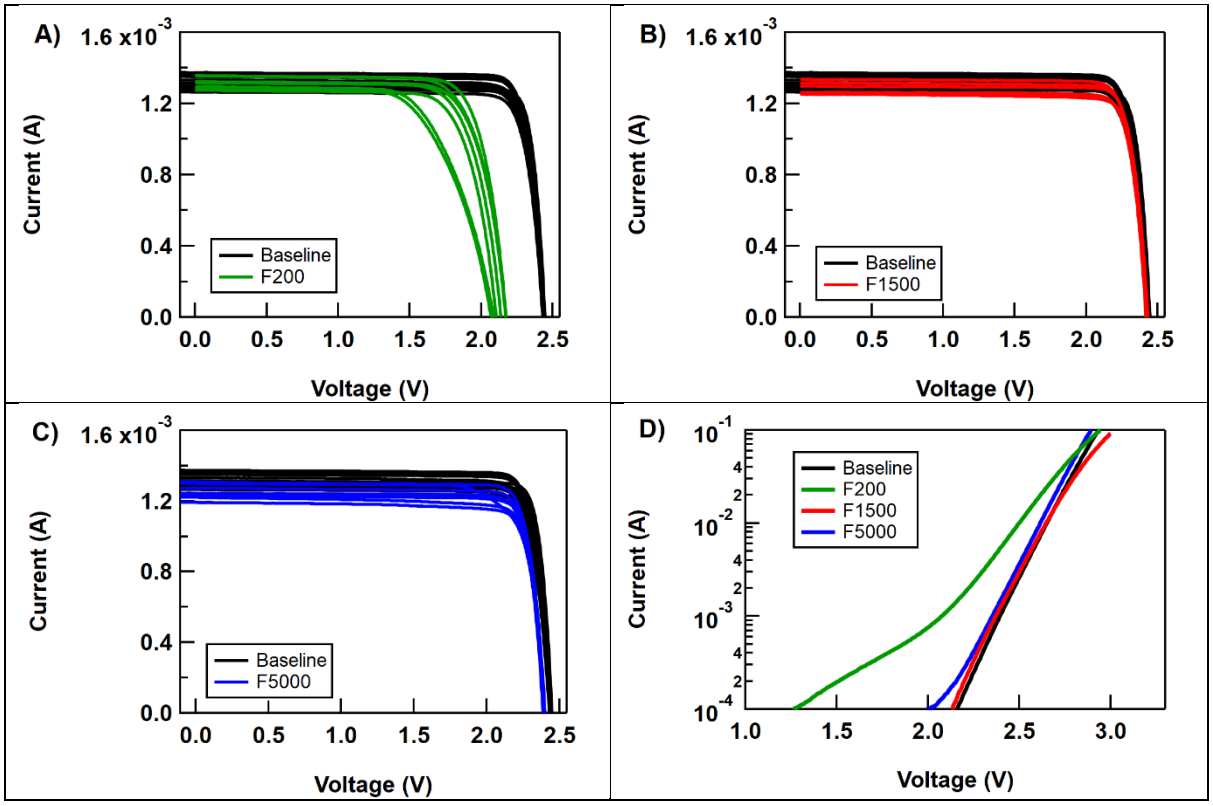

Figure 15 | Light I-V (A-C) and dark I-V curves (D) of the 3JSCs on baseline Ge substrate and GeON. The light I-V curves are taken without spectral correction using a Xe lamp solar simulator.

In summary, the fabrication of 3JSC on the GeON templates shows virtually identical performance results as compared to standard Ge substrates. It thus demonstrates that these thin

Ge epitaxial foils on GeON substrates have the appropriate quality to replace thick Ge wafers as bottom cells and seed for III-V multijunction solar cell fabrication. The motivation for the concept relies however on the foil detachability, which is reported in the next section.

4.3 | Solar cell detachment

The 3JSC detachment was performed by manually transferring the stack to Kapton tape. First, a test structure with the 7-µm Ge foil F1500 and III-V stack grown by MOCVD was transferred to free-standing Kapton tape (**Figure 16 a**). To facilitate the release at the foil edges, the GeON area was pre-scribed prior to the Kapton tape application and peeling. The complete foil area was detached but the tape's small radius of curvature led to cracking, perpendicularly to the detachment direction. This result demonstrates that the GeON detachment layer stayed intact after the high temperature step of MOCVD growth. In the next stage, to detach the F1500 sample with solar cells, the Kapton itself was glued to a glass slide, to prevent bending during peeling. Unfortunately, this also reduced the detachment pressure on the crack front and, as a result, the foil did not detach as a whole piece (**Figure 16 b**). Although layer transfer would require dedicated developments, this result demonstrates that the GeON detachment layer can be adapted to withstand III-V solar cell processing without cracking or flaking.

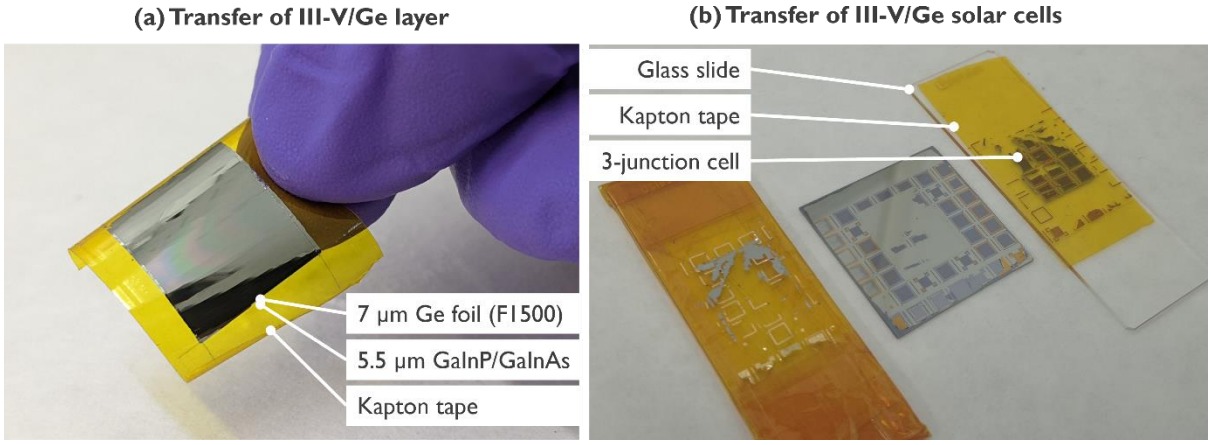

Figure 16 | (a) 19 mm × 15 mm III-V/Ge stack with detachment force F1500 manually transferred to free-standing Kapton tape. (b) Similar stack processed into solar cells transferred in two steps to Kapton tape on a glass slide. The glass slide prevented bending and cracking of the layers but also decreased the pressure applied to the crack front, preventing a complete detachment on the first trial.

5 | Conclusion

This work focused on demonstrating that GeON wafers can ensure the 3-fold functions of Ge wafers for space PV: epi-ready surface for high-quality III-V growth, support carrier for solar cell processing, and bottom solar cell for high-efficiency multijunction. The GeON structure

was upscaled from areas of a few cm^2 to wafer areas, with the transfer of a 11 cm × 11 cm foil to glass. Our process, based on deep-UV lithography, was limited by the wafer in-plane flatness (SFQR). To enable fabricating thicker foils for higher-current bottom junctions, we developed a new epitaxial growth process based on $GeCl_4$. Foils, intrinsic or boron doped, up to 15 µm thickness were grown and growth rates up to 190 nm/min were achieved, which could possibly be pushed further for growing free-standing layers. By reloading the GeON wafer in the epitaxial reactor, the thickness was further increased and foils of 31 µm thickness were detached. To enable safe processing into solar cells, the porous structure was engineered to integrate pillars of controlled width and density, giving control on the detachment force to accommodate the stress induced by the subsequent III-V epitaxy and solar cell process. These pillars do not appear to negatively affect the homo- or hetero-epitaxial properties. 18 different combinations of pillar types and pitches were tested to select foils that could withstand the solar cell process steps, including chemical-vapor deposition for surface passivation and lattice-matched GaInP epitaxy. Triple-junction solar cells GaInP/GaInAs/Ge were fabricated on GeON substrates of 7 µm thickness with 3 different pillar densities. Apart from one sample that was affected by surface debris caused by laser-dicing and ageing defects, no differences in terms of III-V layer nucleation could be detected. In terms of EQE and I-V, no significant differences were found either, except for the lower IR absorption and a 10% lower V_{OC} that can be attributed to the layer thinness and absence of passivation of the foil rear surface. To demonstrate detachability, the layers were then peeled off from the Ge wafer with Kapton tape. In the future, a dedicated solar cell process for detachable foils should be developed, including an optimised layer transfer method, to demonstrate detached wafer-scale solar cells. Another effort could be focused on using a lower-cost lithography, since deep-UV lithography is not a necessity and I-line lithography or nano-imprint may be used – the latter being more tolerant to topography imperfections. In parallel, suitable wafer reconditioning conditions have been found and multiple substrate re-uses may then be demonstrated. Yet, at present, the results above show that it is possible to gain control on the GeON detachability and upscale the concept to areas relevant for the space PV industry. They hence bring the GeON approach beyond proof-of-concept, proving that porous germanium is a serious candidate for replacement of Ge wafers for a more sustainable multijunction solar cell process, with lower germanium waste.

Acknowledgments

At imec, Dirk Rondas and Mustafa Ayyad are gratefully acknowledged for, respectively, processing at the epitaxial reactor and measurements by SIMS.

This project was carried out under a programme of and funded by the European Space Agency (ESA) with contract no. 4000129924/20/NL/FE. The view expressed herein can in no way be taken to reflect the official opinion of the European Space Agency. Funding from Spanish AEI (projects RTI2018-094291-B-I00, PID2021-123530OB-I00) is gratefully acknowledged. This publication is part of the project EQC2019-005701-P, funded by AEI/ 10.13039/501100011033, MCIN and ERDF "A way to make Europe". V. Orejuela is funded by the Spanish Ministerio de Ciencia e Innovación (MICINN) through a FPI grant (PRE2019-088437).

References

[1] European Commission, "Critical Raw Materials Resilience: Charting a Path towards greater Security and Sustainability." Mar. 09, 2020. [Online]. Available: https://eur-lex.europa.eu/legal-content/EN/TXT/PDF/?uri=CELEX:52020DC0474&from=EN

[2] Y. A. Bioud *et al.*, "A porous Ge/Si interface layer for defect-free III-V multi-junction solar cells on silicon," in *Physics, Simulation, and Photonic Engineering of Photovoltaic Devices VIII*, Feb. 2019, vol. 10913, p. 109130T. doi: 10.1117/12.2511080.

[3] I. García *et al.*, "Ge virtual substrates for high efficiency III-V solar cells: applications, potential and challenges," in *2019 IEEE 46th Photovoltaic Specialists Conference (PVSC)*, Jun. 2019, pp. 1444–1451. doi: 10.1109/PVSC40753.2019.8980914.

[4] I. García, L. Barrutia, S. Dadgostar, M. Hinojosa, A. Johnson, and I. Rey-Stolle, "Thinned GaInP/GaInAs/Ge solar cells grown with reduced cracking on Ge|Si virtual substrates," *Solar Energy Materials and Solar Cells*, vol. 225, p. 111034, Jun. 2021, doi: 10.1016/j.solmat.2021.111034.

[5] M. Ghosh *et al.*, "Ultrathin Ge epilayers on Si produced by low-temperature PECVD acting as virtual substrates for III-V / c-Si tandem solar cells," *Solar Energy Materials and Solar Cells*, vol. 236, p. 111535, Mar. 2022, doi: 10.1016/j.solmat.2021.111535.

[6] S.-H. Bae *et al.*, "Integration of bulk materials with two-dimensional materials for physical coupling and applications," *Nat. Mater.*, vol. 18, no. 6, Art. no. 6, Jun. 2019, doi: 10.1038/s41563-019-0335-2.

[7] J. S. Ward *et al.*, "Techno-economic analysis of three different substrate removal and reuse strategies for III-V solar cells," *Progress in Photovoltaics: Research and Applications*, vol. 24, no. 9, pp. 1284–1292, 2016, doi: 10.1002/pip.2776.

[8] pv magazine, "Something truly new," *pv magazine International*, Jan. 06, 2021. https://www.pv-magazine.com/magazine-archive/something-truly-new/ (accessed Jan. 06, 2021).

[9] N. Milenkovic *et al.*, "20% efficient solar cells fabricated from epitaxially grown and freestanding n-type wafers," *Solar Energy Materials and Solar Cells*, vol. 159, pp. 570–575, Jan. 2017, doi: 10.1016/j.solmat.2016.09.044.

[10] S. Park *et al.*, "Germanium-on-Nothing for Epitaxial Liftoff of GaAs Solar Cells," *Joule*, vol. 3, no. 7, pp. 1782–1793, Jul. 2019, doi: 10.1016/j.joule.2019.05.013.

[11] G. Courtois *et al.*, "Development of germanium-on-germanium engineered substrates for III-V multijunction solar cells," in *2020 47th IEEE Photovoltaic Specialists Conference (PVSC)*, Jun. 2020, pp. 1053–1055. doi: 10.1109/PVSC45281.2020.9300462.

[12] N. Paupy *et al.*, “Epitaxial growth of detachable GaAs/Ge heterostructure on mesoporous Ge substrate for layer separation and substrate reuse,” presented at the 49th IEEE Photovoltaic Specialists Conference, Philadelphia, Jun. 2022.
[13] N. Paupy *et al.*, “Wafer-scale detachable mono-crystalline Ge nanomembranes for the growth of III-V materials and substrate reuse,” *Advanced Materials*, submitted.
[14] T. Sato *et al.*, “Fabrication of Silicon-on-Nothing Structure by Substrate Engineering Using the Empty-Space-in-Silicon Formation Technique,” *Japanese Journal of Applied Physics*, vol. 43, no. No. 1, pp. 12–18, Jan. 2004, doi: 10.1143/JJAP.43.12.
[15] M. G. Jeong, T. Kim, B. J. Lee, and J. Lee, “Thick Germanium-on-Nothing Structures by Annealing Microscale Hole Arrays With Straight Sidewall Profiles,” *Journal of Microelectromechanical Systems*, pp. 1–3, 2022, doi: 10.1109/JMEMS.2021.3139094.
[16] I. Lombardero, M. Ochoa, N. Miyashita, Y. Okada, and C. Algora, “Theoretical and experimental assessment of thinned germanium substrates for III–V multijunction solar cells,” *Progress in Photovoltaics: Research and Applications*, vol. 28, no. 11, pp. 1097–1106, 2020, doi: 10.1002/pip.3281.
[17] R. Kurstjens *et al.*, “GaInP solar cells grown on Ge-on-Ge engineered substrates,” in *2021 IEEE 48th Photovoltaic Specialists Conference (PVSC)*, Jun. 2021, pp. 0175–0177. doi: 10.1109/PVSC43889.2021.9518407.
[18] H. Sivaramakrishnan Radhakrishnan *et al.*, “Kerfless layer-transfer of thin epitaxial silicon foils using novel multiple layer porous silicon stacks with near 100% detachment yield and large minority carrier diffusion lengths,” *Solar Energy Materials and Solar Cells*, vol. 135, no. Supplement C, pp. 113–123, Apr. 2015, doi: 10.1016/j.solmat.2014.10.049.
[19] I. Massiot, A. Cattoni, and S. Collin, “Progress and prospects for ultrathin solar cells,” *Nat Energy*, vol. 5, no. 12, pp. 959–972, Dec. 2020, doi: 10.1038/s41560-020-00714-4.
[20] J.-S. Park, M. Curtin, C. Major, S. Bengtson, M. Carroll, and A. Lochtefeld, “Reduced-Pressure Chemical Vapor Deposition of Epitaxial Ge Films on Si(001) Substrates Using GeCl4,” *Electrochem. Solid-State Lett.*, vol. 10, no. 11, p. H313, Aug. 2007, doi: 10.1149/1.2771069.
[21] D. McDermott *et al.*, “Germanium epitaxy using GeCl4: growth kinetics and material properties,” presented at the 2021 European Material Research Society (E-MRS) Fall meeting, Warsaw, 2021. [Online]. Available: https://www.european-mrs.com/integration-advanced-materials-silicon-classical-neuromorphic-and-quantum-applications-emrs-0
[22] R. Loo *et al.*, “High Quality Ge Virtual Substrates on Si Wafers with Standard STI Patterning,” *J. Electrochem. Soc.*, vol. 157, no. 1, p. H13, Nov. 2009, doi: 10.1149/1.3244564.
[23] G. Wang *et al.*, “A model of threading dislocation density in strain-relaxed Ge and GaAs epitaxial films on Si (100),” *Appl. Phys. Lett.*, vol. 94, no. 10, p. 102115, Mar. 2009, doi: 10.1063/1.3097245.
[24] V. Terzieva *et al.*, “Benefits and side effects of high temperature anneal used to reduce threading dislocation defects in epitaxial Ge layers on Si substrates,” *Thin Solid Films*, vol. 517, no. 1, pp. 172–177, Nov. 2008, doi: 10.1016/j.tsf.2008.08.144.
[25] R. Loo *et al.*, “Epitaxial Ge Virtual Substrates and Ge-on-Nothing on Si: Comparison of Material Properties,” 2022.
[26] J. Cho *et al.*, “GeCl4-based High Quality Ge epitaxy on Engineered Ge Substrates for Thin Multi-junction Solar Cells,” presented at the 2022 IEEE 49th Photovoltaic Specialists Conference (PVSC), Jun. 2022.
[27] Y. N. Picard *et al.*, “Future Prospects for Defect and Strain Analysis in the SEM via Electron Channeling,” *Microscopy Today*, vol. 20, no. 2, pp. 12–16, Mar. 2012, doi: 10.1017/S1551929512000077.

[28] L. Barrutia *et al.*, “Development of the Lattice Matched GaInP/GaInAs/Ge Triple Junction Solar Cell with an Efficiency Over 40%,” in *2018 Spanish Conference on Electron Devices (CDE)*, Nov. 2018, pp. 1–4. doi: 10.1109/CDE.2018.8596996.